Journal of Fluorescence, Vol. 2, No. 1, 1992

Simultaneous Registration of Ca^{2+} Transients and Volume Changes in Rat Mesangial Cells: Evaluation of the Effects of Protein Kinase C Down-Regulation[1]

Martin Ochsner,[2,6] Thomas Fleck,[3] Peter Kernen,[4] David A. Deranleau,[4] and Josef Pfeilschifter[5]

Received December 5, 1991; revised March 30, 1992; accepted March 31, 1992

The intracellular free Ca^{2+} concentration ($[Ca^{2+}]_i$) could be correlated with the contractile response in rat mesangial cells using an apparatus which measured both biochemical processes simultaneously. Long-term pretreatment of mesangial cells with 12-*O*-tetradecanoly-phorbol 13-acetate (24 h, 500 n*M*) increased the (20 n*M*) angiotensin II-induced mobilization of Ca^{2+} and led to an enhanced and sustained contraction of the cells. The contractile response was delayed by approximately 3.5 s with respect to the intracellular increase in Ca^{2+} concentration. The simultaneous registration of Ca^{2+} transients and cell contractions confirms that $[Ca^{2+}]_i$ is the major determinant of the angiotensin II-mediated mesangial cell contraction.

KEY WORDS: Angiotensin II; Ca^{2+}; protein kinase C; 12-*O*-tetradecanoyl-phorbol 13-acetate (TPA); contraction of mesangial cells.

INTRODUCTION

Mesangial cells play a dominant role in the regulation of the glomerular filtration rate. Morphologically, they closely resemble vascular smooth muscle cells. Vasoactive hormones, such as angiotensin II and vasopressin, cause an immediate activation of phospholipase C which triggers the breakdown of phosphoinositides and the intracellular release of inositol-1,4,5-tris-phosphate ($InsP_3$) and diacylglycerol (DAG). $InsP_3$ mobilizes Ca^{2+} from internal stores and DAG activates protein kinase C (PKC). The interplay of these intracellular messengers mediates a wide variety of cellular responses (1).

As we have shown previously, a long-term pretreatment of mesangial cells with the phorbolester 12-*O*-tetradecanoyl-phorbol 13-acetate (TPA) leads to a down-regulation of the protein kinase C activity and results in elevated, angiotensin II-stimulated levels of $InsP_3$ and intracellular free Ca^{2+} $[Ca^{2+}]_i$ (2,3). Subsequent microscopic measurements further indicated that the contractile response of TPA-pretreated mesangial cells is significantly amplified with respect to control cells (2). Due to the discontinuous measurement technique used, however, it was impossible until now to get an insight into the sequence and dynamic nature of the induced biological processes.

To establish a correlation between the intracellular Ca^{2+} concentration (4–8) and the cell volume (9,10), we used an apparatus which is capable of measuring both

[1] Dedicated to Professor Horst H. A. Linde on the occasion of his 60th birthday.

[2] CIBA-GEIGY Ltd., Photophysics Department, Postfach, CH-4002 Basle, Switzerland.
[3] Pharmaceutical Institute, University of Basle, CH-4051 Basle, Switzerland.
[4] Theodor Kocher Institute, University of Bern, CH-3000 Bern 9, Switzerland.
[5] Biocenter, Department of Pharmacology, University of Basle, CH-4056 Basle, Switzerland.
[6] To whom correspondence should be addressed.

1053-0509/92/0300-0037$06.50/0

biological processes simultaneously. The registration of the $[Ca^{2+}]_i$ transient is based on the spectroscopic determination of the free and Ca^{2+}-bound concentration of the Ca^{2+}-indicator indo-1 (11,12). The cell volume is obtained by measuring the transmitted light intensity at a wavelength which is not absorbed by cellular components and by relating the calculated absorbance to the theoretical scattering cross section.

EXPERIMENTAL

Materials

HEPES [4-(2-hydroxyethyl)-piperazine-1-ethanesulfonate] and TPA were from Sigma, St. Louis, MO; indo-1:AM was from Molecular Probes Inc., Eugene, OR; angiotensin II and ionomycin were from Calbiochem, Lucerne, Switzerland; and EGTA was from Fluka, Buchs, Switzerland. All other chemicals were purchased from Merck, Darmstadt, FRG.

Methods

Cell Culture

Rat mesangial cells were cultivated essentially as described previously (2,13). The cells were grown in RPMI 1640 medium (supplemented with 10% fetal calf serum), morphologically characterized by phase-contrast microscopy, and differentiated from endothelial and epithelial contaminations.

Prior to the spectroscopic measurements one fraction of the cultivated cells was incubated with 500 n*M* TPA for 24 h.

Cell Labeling with Indo-1

In order to standardize the incubation procedure, aliquots of the mesangial cell suspension (10^7 cells/ml) were loaded separately with indo-1:AM (1 μ*M*, 20 min, 37°C) in the presence of $CaCl_2$ (1.3 m*M*). At the end of the incubation interval the cells were centrifuged (70*g*, 5 min, 25°C) and resuspended in buffer medium to yield a final concentration of 10^6 cells/ml. The buffer medium contained the following ingredients at physiological concentrations: 1.3 m*M* $CaCl_2$, 135 m*M* NaCl, 5 m*M* KCl, 1 m*M* Na_2HPO_4, 1 m*M* $MgCl_2$, and 5 m*M* *d*-glucose, buffered to a pH of 7.4 with 10 m*M* HEPES/HCl.

Experimental Technique for the Simultaneous Measurements of $[Ca^{2+}]_i$ Transients and Shape Changes

The optical layout of the apparatus is schematically displayed in Fig. 1.

Fluorescence spectra and light transmission were recorded simultaneously using a multichannel analyzer and dedicated photodiodes (14). The 356.4-nm line of a krypton ion laser (Coherent Model Innova 90k) was selected to excite the intracellular calcium indicator indo-1 near its isosbestic point, and the calcium concentration-dependent fluorescence spectra were acquired at the polychromator exit plane by means of an intensified linear diode array camera (512 pixels, Princeton Applied Research Model 1420N). Background spectra (autofluorescence from unlabeled control cells plus a small diode dark signal) were automatically subtracted.

Light transmission measurements were made at 632.8 nm, where mesangial cells scatter but do not absorb, using a vertically polarized, frequency-stabilized He/Ne laser (Coherent Model 200). The laser beam was expanded to a Gaussian (1/*e*) diameter of 6 mm to increase the number of cells under observation and crossed unfocused the thermostated (25°C) and magnetically stirred 1-cm standard sample cuvette. All transmission measurements were carried out in ratio mode [transmission $T = I(t)/I_O$, where I_O gives the incident and $I(t)$ the transmitted intensity as a function of time]. To isolate the He/Ne wavelength, two interference filters (Corion, IF filter = 632.8 nm, FWHM = 1 nm) were used as indicated in Fig. 1 in front of reference and transmitted light detectors (EG&G UV-444B photodiodes). A small (1-mm-diameter) iris placed in front of the transmission detector was used to prevent forward-scattered light from the cells from reaching the detector.

The increase in the intracellular free Ca^{2+} concentration and the alteration of the cell volume were triggered by an injection of angiotensin II (20 n*M*) in both the TPA-pretreated and the control cell group. The time required for a homogeneous distribution of the injected angiotenin II in the sample cuvette was about 0.5 s, which limits the maximum time resolution of the experiment.

At the end of each experiment the Ca^{2+} ionophore ionomycin (1 μ*M*) was added to equilibrate the extracellular and intracellular Ca^{2+} levels (11) and to induce a sustained contraction of the cells. To calibrate the volume changes an aliquot of the cell suspension was mi-

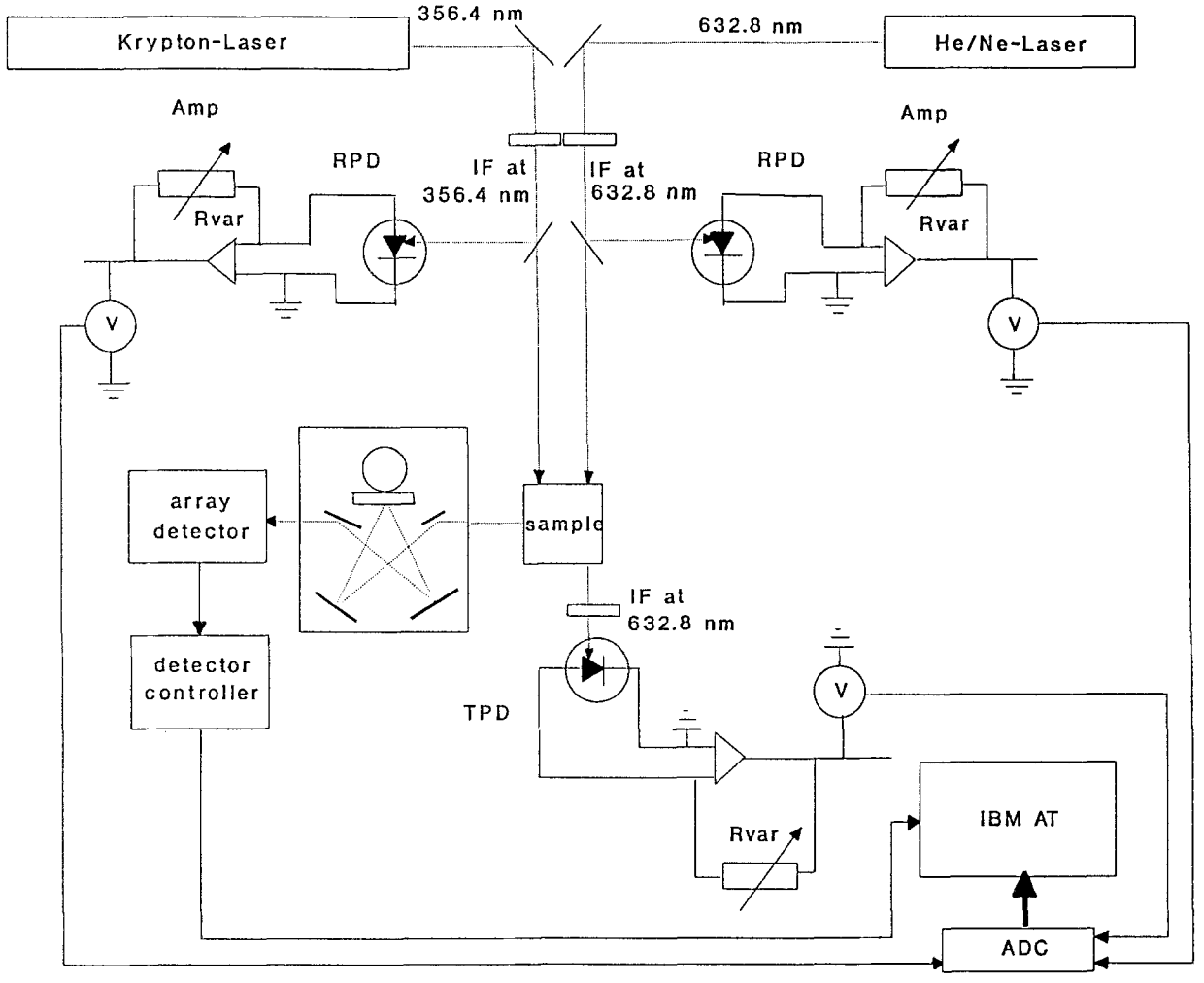

Fig. 1. Schematic experimental setup for the simultaneous measurement of intracellular Ca^{2+} concentrations and cell volumes. IF, interference filter; RPD, reference photodiode; Amp, amplifier; Rvar, variable resistance; TPD, transmission photodiode; ACD, analog-to-digital converter.

croscopically analyzed and the actual cell volume determined.

RESULTS

Ca^{2+} Measurements

Mathematical Model for Analyzing Ca^{2+} Transients

The intracellular Ca^{2+} concentrations were calculated from the ratio of the fluorescence emissions at 405 and 475 nm according to the guidelines given by Grynkiewicz *et al.* (11).

A modified Bateman function was used to fit the experimental data and obtain physiologically meaningful constants which characterize the Ca^{2+} transient. The model takes an exponential behavior into account as follows:

$$[Ca^{2+}]_i(nM) = C1[2^{(-(t-t_0)/\gamma_{el})} - 2^{-(t-t_0)/\gamma_{in1})}] + C2\,[1 - 2^{(-(t-t_0)/\gamma_{in2})}] + C3 \quad (1)$$

The parameters C1 (n*M*) and C2 (n*M*) correspond to the maximal increase in the intracellular Ca^{2+} concentration induced by $InsP_3$ and by an influx of Ca^{2+}, respectively. The onset of the Ca^{2+} release is given t_O (s). γ_{el} (s) characterizes the Ca^{2+} half-life elimination constant, and γ_{in1} (s) and γ_{in2} (s) the half-life rise times of the individual Ca^{2+} channel increases. Finally, C3 (n*M*) corresponds to the basal Ca^{2+} level.

The fitting function is based on the idea that two different processes are dominating the release and reup-

take of Ca^{2+}. The first mechanism [first term in Eq. (1)] characterizes the $InsP_3$-induced intracellular liberation of Ca^{2+}. The second term in Eq. (1) corresponds to the rise in intracellular Ca^{2+} concentration caused by a stimulus-induced increase in the permeability of the calcium channels located in the plasma membrane (2).

The Influence of TPA Pretreatment on the Intracellular Ca^{2+} Transients

In general, our calcium results (Table I and Figs. 2 and 3, top panels) are in good agreement with our previous data (2). As we have shown hitherto, the intracellular release of Ca^{2+} is mediated mainly by an increase in the intracellular $InsP_3$ concentration (2). Long-term pretreatment with TPA had no significant effect on the basal calcium concentration but amplified the angiotensin II-induced increase in the intracellular calcium concentration by typically 25%. All calcium transients from TPA-pretreated cells revealed nonexponential decay characteristics, indicating that the interaction with angiotensin II leads to an elevated steady-state level of $[Ca^{2+}]_i$ (at least within the time frame of our experiment).

For TPA-pretreated cells, the elimination of Ca^{2+} from the cytoplasm (as characterized by the parameter γ_{el}) was significantly delayed compared to control cells (see Table I). Yet the absolute values of the elimination constants published by Pfeilschifter *et al.* (2) imply that the liberated Ca^{2+} ions were sequestered much more rapidly under our experimental conditions. A possible reason for this discrepancy may be that calcium buffering by indo-1 was significantly reduced because a much lower concentration of indicator was used in the present study (the length of the incubation period was shortened in our experiments to minimize the amount of the indicator that entered the cells). At any rate, our results clearly indicate that the absolute values of elimination constants obtained by various laboratories under different conditions are not necessarily comparable. Thus reliable conclusion can be drawn only if the calculated decay constants are related to those of a control cell group.

Table I. Angiotensin II-Induced Ca^{2+} Release[a]

Constant	Cells	Samples	Mean value	SD
t_o	TPA	6	23.1 s	0.5 s
	Control	6	22.2 s	0.4 s
C1	TPA	4	100 n*M*	5 n*M*
	Control	4	82 n*M*	2 n*M*
C2/C1	TPA	4	8%	1%
	Control	4	4%	1%
γ_{el}	TPA	5	12 s	1 s
	Control	5	8 s	1 s
C3	TPA	5	160 n*M*	15 n*M*
	Control	5	170 n*M*	20 n*M*

[a] All parameters are obtained by fitting the experimental data to the following function (for an explanation, see the text): $[Ca^{2+}]_i(nM) = C1[2^{(-(t-to)/\gamma el)} - 2^{(-(t-to)/\gamma in1)}] + C2\,[1 - 2^{(-(t-to)/\gamma in2)}] + C3$. C1; γ_{in1} = maximal increase in the intracellular Ca^{2+} concentration (n*M*) and half-life rise time (s) characteristic for $InsP_3$-mediated effects. C2; γ_{in2} = maximal increase in the intracellular Ca^{2+} concentration (n*M*) and half-life rise time (s) characterizing the Ca^{2+} influx. t_o = onset of Ca^{2+} release (s). γ_{el} = Ca^{2+} half-life elimination constant (s). C3 = Ca^{2+} basis level (n*M*).

Volume Changes

Mathematical Model for Analyzing Volume Changes

The light scattered by a biological object is related to its size, shape, and refractive index relative to those of the surrounding medium. The criterion as to which scattering theory applies depends mainly on the particle size factor $x = 2\pi r/\lambda$ (ratio between particle radius r and excitation wavelength λ) and on the phase shift factor $p = 2x(m-1)$, where $m = n/n_0$ is the ratio of the refractive indices of cell medium and solvent (15).

Cultivated mesangial cells are spherical, with a typical diameter of 30 μm and a refractive index of 1.37 (M. Ochsner, T. Fleck, and D. A. Deranleau, unpublished data). Microscopic measurements indicated that ionomycin causes no deviation from spherical symmetry. Following the recommendation of van de Hulst (15), the particles can therefore be appropriately characterized by anomalous diffraction theory [$x >> 1$ and $(m-1) << 1$]. Low particle concentrations (10^6/ml) were used to minimize multiple scattering.

Neglecting any light which might be absorbed by the cells at the He/Ne laser frequency, the extinction of the suspension is related to the decadic scattering extinction coefficient $\epsilon_s(t)$ by Beer's law:

$$E(t) = -\log[T(t)] = \epsilon_s(t) * c_o * d \qquad (2)$$

where $E(t)$ and $T(t)$ correspond, respectively, to the experimentally determined absorbance and transmission data as a function of time. c_0 gives the concentration of cells, and d the thickness of the cuvette.

The relationship between the scattering coefficient $\epsilon_s(t)$ of a spherical particle and the apparent cell volume

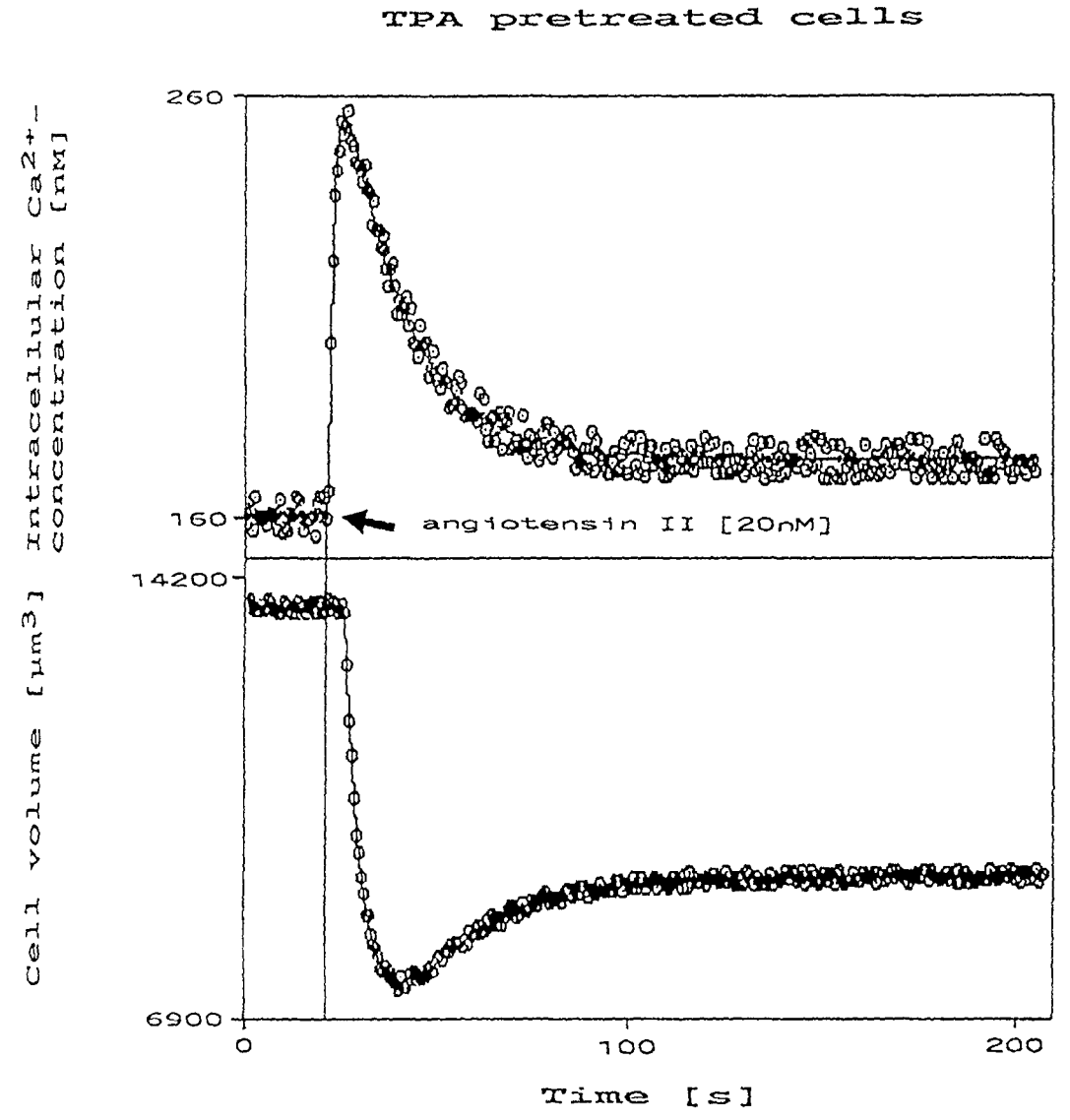

Fig. 2. Ca^{2+} response and volume contraction of TPA-pretreated cells. The (20 n*M*) angiotensin II-induced Ca^{2+} response (top) is presented simultaneously with the variation of its cell volume (bottom). The *X* axis corresponds in both figures to the time scale. The *Y* axis in the top panel gives the intracellular Ca^{2+} concentration; the *Y* axis in the bottom panel, the apparent cell volume. Dotted points correspond to the experimentally observed data; the line, to the theoretically predicted transients by using the model functions as given in text. One can estimate a time lag of approximately 3.5 s between the onset of Ca^{2+} release and the initiation of the volume change.

is obtained by integrating the angular scattering intensities over the surface of a sphere (15):

$$\epsilon_s(t) \propto (n_{cell}(t)/n_{water} - 1)^2 * V(t)^{4/3}/\lambda^2 \qquad (3)$$

n_{water} and $n_{cell}(t)$ characterize, respectively, the refractive indices of water and of cells as a function of time. $V(t)$ gives the time-dependent cell volume and λ corresponds to the wavelength of the He/Ne laser (632.8 nm).

As indicated in Eq. (3), the scattering coefficient $\epsilon_s(t)$ is proportional to the 4/3 power of the cell volume and varies as the inverse square of the wavelength.

Based on the assumption that the refractive index of mesangial cells $[n_{cell}(t)]$ does not change considerably during the process of contraction, the extinction is directly related to the cell volume according to

$$E(t) = k_1(n_{cell}, c_o, \lambda) * V(t)^{4/3} \qquad (4)$$

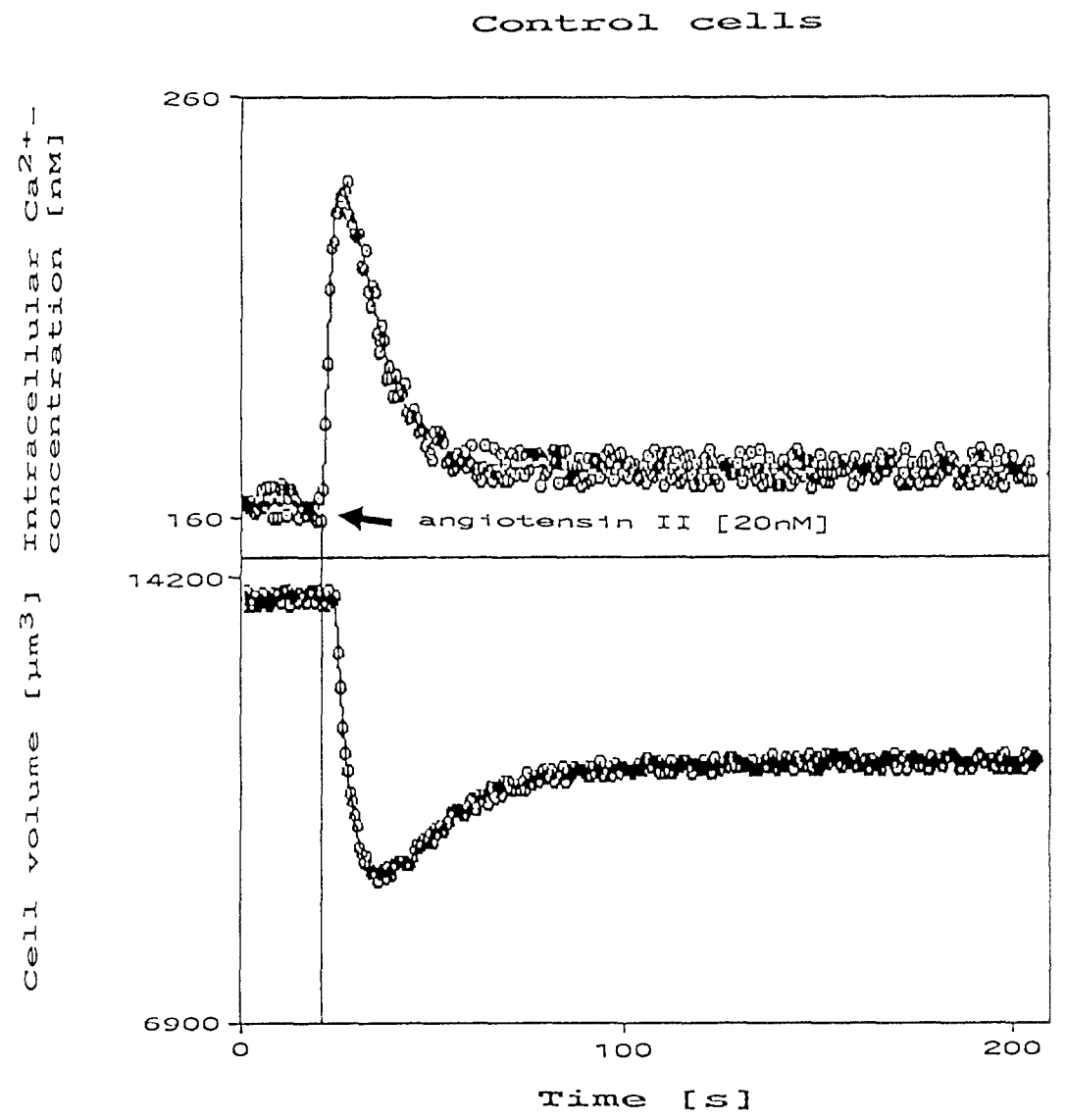

Fig. 3. Ca^{2+} response and volume contraction of control cells. In parallel to Fig. 2, the (20 n*M*) angiotensin II-induced Ca^{+} response (top) of control cells is presented simultaneously with the variation of its cell volume (bottom).

The constant k_1 (n_{cell},c_0, λ) in Eq. (4) was calculated from the first experimental data point [$E(t=0)$] by taking account of the microscopically determined cell volume (V_o):

$$k_1(n_{cell}, c_o, \lambda) = E(t = 0)/V_o^{4/3} \quad (5)$$

Subsequently all absorbance data were numerically fitted to Eq. (4) and the cell volume together with its derivative (=speed of contraction) calculated as a function of time (see Table II).

As mentioned above, ionomycin was added at the end of each experiment to equilibrate the extra- and intracellular Ca^{2+} concentrations and to induce a sustained contraction. In order to test the mathematical model used, an aliquot of the cell suspension was analyzed on a high-precision microscope (Reichert-Jung Polyvar MET) by measuring the diameter of 100 cells before and after the addition of ionomycin. The theoretically predicted and microscopically determined and averaged cell volumes of both native and ionomycin-pretreated cells were identical within an experimental error of about 5% and indicated that our theoretical model gives reasonable estimates of the actual cell volume.

Table II. Angiotensin II-Induced Volume Changes[a]

Constant	Cells	Samples	Mean value	SD
V_o	TPA	50	14,140 μm³	120 μm³
	Control	50	14,190 μm³	110 μm³
r_o	TPA	50	15.0 μm	0.1 μm
	Control	50	15.0 μm	0.1 μm
Onset of shape change	TPA	6	26.8 s	0.5 s
	Control	6	25.6 s	0.2 s
$[dV/dt]_{max}$	TPA	6	−4570 μm³/s	135 μm³/s
	Control	6	−3550 μm³/s	120 μm³/s
$[dr/dt]_{max}$	TPA	6	−1.6 μm/s	0.1 μm/s
	Control	6	−1.3 μm/s	0.1 μm/s
V_{min}	TPA	6	6985 μm³	80 μm³
	Control	6	9220 μm³	95 μm³
r_{min}	TPA	6	11.9 μm	0.3 μm
	Control	6	13.0 μm	0.4 μm

[a] The symbols V_o and r_o refer to the volume and the radius of mesangial cells determined by microscopic measurements at the beginning of the experiment. All other parameters are obtained by fitting the experimental data to the following function (for an explanation, see the text): $E(t) = k_1(n_{cell}, c_o, \lambda) * V(t)^{4/3}$. V_{min} corresponds to the lowest cell volume being transiently reached by the addition of angiotensin II (20 n*M*). r_{min} gives the cell volume in terms of its radius. $[dV/dt]_{max}$ and $[dr/dt]_{max}$ characterize the maximal speed of contraction.

The Influence of TPA Pretreatment on Shape Changes

Based on the methods outlined above, the variation of the cell volume and the speed of contraction was calculated as a function of time for TPA-pretreated and control cells (see bottom panels in Figs. 2–4).

The numerical parameters which characterize the displayed curves are summarized in Table II and reveal significant differences between TPA-pretreated cells and control cells. TPA-pretreated cells contracted faster (+30%) and more strongly (+40%). As can be seen from Figs. 2 and 3, contracted cells remain in a contracted state, relaxing only slightly within the time frame of the experiment. The final cell volume was in good agreement with our previous microscopic data (2). However, pretreatment with TPA had no significant effect on the time delay (≈3.5 s) between Ca^{2+} release and contractile response (see Table III).

DISCUSSION

The simultaneous registration of Ca^{2+} transients and of transmission changes offers an insight into the sequence and dynamics of the induced biological processes. The contraction of the cell was delayed by approximately 3.5 s with respect to the onset of the Ca^{2+} release (see Table III). No significant differences were found between the cell groups, indicating that pretreatment with TPA does not influence the sensitivity of the contractile components to Ca^{2+}. As outlined above, TPA-pretreated cells contract faster and more strongly compared to control cells, which indicates a close relationship between the angiotensin II-induced volume contraction and its associated speed of contraction.

The contraction was almost completely inhibited by pretreating the cells with EGTA (2 m*M*, 15 min; data not shown). In contrast to the pseudopod extension reaction in neutrophils (D. A. Deranleau, personal communication), an increase in the intracellular Ca^{2+} concentration was required to induce the contractile reaction. Analogous to its function in smooth muscle cells, Ca^{2+} is assumed to occupy a central role in excitation contraction coupling in mesangial cells. Agonist-stimulated $InsP_3$ formation and Ca^{2+} mobilization initiates a number of Ca^{2+}-calmodulin-dependent processes, including activation of myosin light-chain kinase, with subsequent phosphorylation of 20-kDa myosin light chains. Phosphorylation of smooth muscle myosin is associated with an activation of its actin-related ATPase activity which ultimately leads to tension development (16). In the continuous presence of an agonist, myosin light-chain phosphorylation is transient, although a constant level of isometric force is maintained. This indicates that additional Ca^{2+}-dependent regulatory events must be involved in sustained contraction. Rasmussen *et al.* (17) suggested that PKC-mediated phosphorylation of structural and regulatory components of the filamin–actin–desmin fibrillar domain may be responsible for sustained smooth muscle contraction. In addition, Troyer *et al.* (18) reported that phorbol ester causes a slow contraction of mesangial cells. Much to our surprise, the contractile response of mesangial cells to a challenge with angiotensin II was potentiated in PKC-depleted cells compared to control cells (this paper and Ref. 2). These results show that Ca^{2+} is the major determinant of angiotensin II-induced mesangial cell contraction. The contribution of PKC is an inhibitory one, leading to a rapid desensitization of the hormone-stimulated signaling events. Recently, it has been reported that a hormone-stimulated K^+ depolarization of smooth muscle causes myosin light-chain phosphorylation at a single site, corresponding to a myosin light-chain kinase phosphorylation, with no phosphorylation at PKC sites of the myosin light chain (19,20). Furthermore, this site of phosphorylation is sufficient for contraction, thus strongly suggesting that PKC plays no physiological role in maintaining tonic force by regulating the level of myosin light-chain phosphorylation.

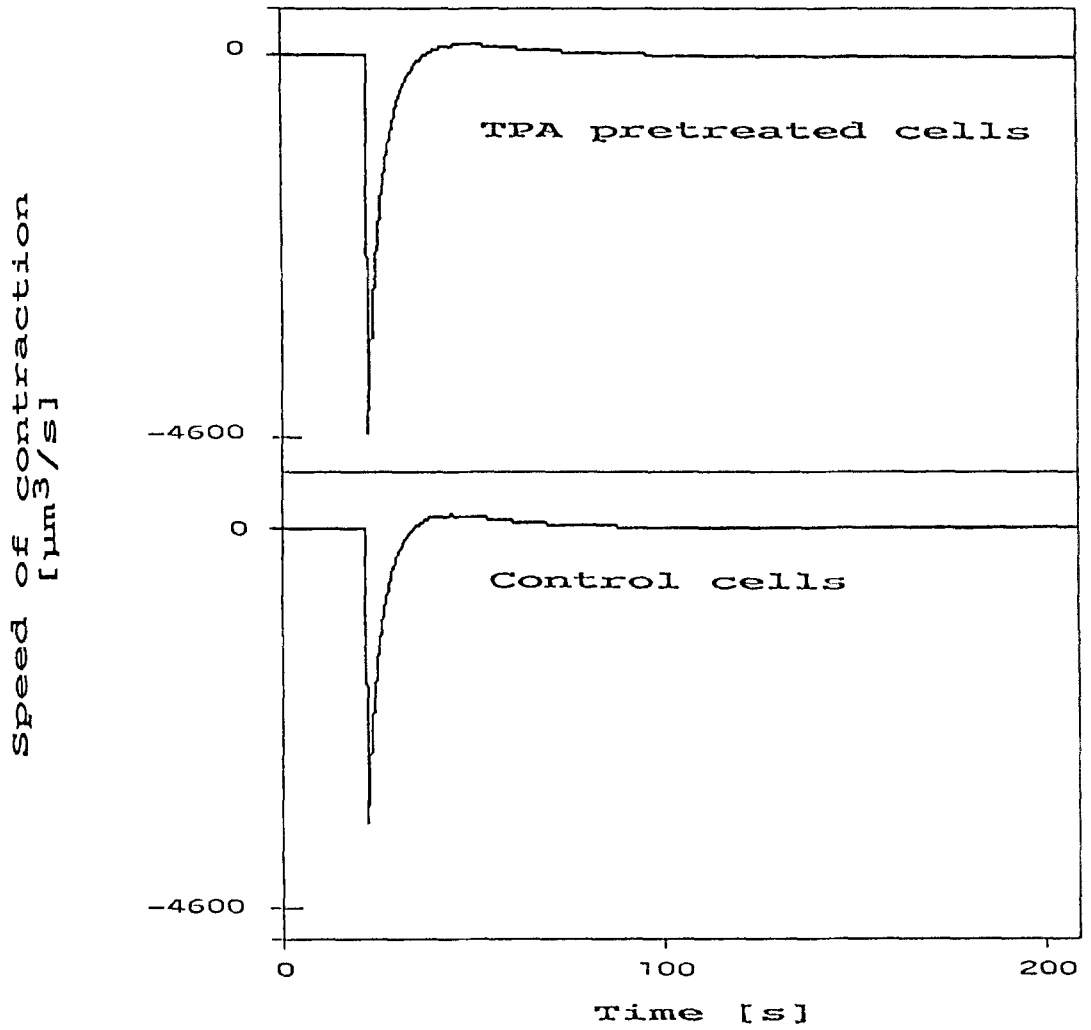

Fig. 4. Speed of contraction of TPA-pretreated and control cells as a function of time. The *X* axis corresponds to the time scale. The *Y* axis gives the speed of contraction ($\mu m^3/s$). The associated maximum amplitude, which refers to the maximum speed of contraction, for TPA-pretreated cells is significantly larger (by 30%) than that for the control cell group.

Table III. Time Delay between Ca^{2+} Release and Volume Contraction

			Seconds	
Constant	Cells	Samples	Mean	SD
Time delay	TPA	6	3.7	0.4
	Control	6	3.4	0.3

Obviously, the dominant role of PKC is to exert a stringent negative feedback control on hormone-induced mesangial cell contraction. PKC is a family of at least eight isoenzymes, all having closely related structures but differing in tissue and cellular distribution (21). Very recently, we have obtained evidence suggesting that PKC-α mediates feedback inhibition of inositol lipid turnover in mesangial cells (22).

ACKNOWLEDGMENT

We wish to thank Mr. Victor Crea for his technical assistance.

REFERENCES

1. Pfeilschifter, J. 1990. *Klin. Wochenschr.* **68**, 1134–1137.
2. Pfeilschifter, J., Fandrey, J., Ochsner, M., Whitebread, S., and de Gasparo, M. 1990. *FEBS Lett.* **261**, 307–311.
3. Pfeilschifter, J. 1989. *Renal Physiol. Biochem.* **12**, 1–31.
4. Ochsner, M., Creba, J., Walker, J., Bentley, Ph., and Muakassah-Kelly, S. F. 1990. *Biochem. Pharmacol.* **40**, 2247–2257.
5. v. Tscharner, V., Deranleau, D. A., and Baggiolini, M. 1986. *J. Biol. Chem.* **261**, 10163–10168.
6. Meyer, T., Wensel, T., and Stryer L. 1990. *Biochemistry* **29**, 32–37.
7. Merrit, J. E., McCarthy, S., Davies, M. P. A., and Moores, K. E. 1990. *Biochem. J.* **269**, 513–519.
8. Popov, E. G., Garrilov, I. Y., Pozier, E. Y., and Gabbasov, Z. A. 1988. *Arch. Biochem. Biophys.* **261**, 91–96.
9. Fandrey, J. and Jelkmann, W. 1988. *Prostaglandines* **36**, 249–257.
10. Ausiello, D. A., Kreisberg, J. I., Roy, C., and Karnovsky, M. J. 1980. *J. Clin. Invest.* **65**, 754–760.
11. Grynkiewicza, G., Poenie, M., Tsien, R. Y. 1985. *J. Biol. Chem.* **260**, 3440–3450.
12. Tsien, R. Y. 1989. *Annu. Rev. Neurosci.* **12**, 227–253.
13. Pfeilschifter, J., Kurtz, A., and Bauer, C. 1984. *Biochem. J.* **223**, 855–859.
14. Deranleau, D. A., and Stüssi, E. 1987. *Rev. Sci. Instrum.* **58**, 1840–1842.
15. van de Hulst, H. C. 1957. *Light Scattering by Small Particles,* Wiley, New York.
16. Kamm, K. E., and Stull, J. T. 1985. *Annu. Rev. Pharmacol. Toxicol.* **25**, 593–620.
17. Rasmussen, H., Takuwa, Y., and Park, S. 1987. *FASEB J.* **1**, 177–185.
18. Troyer, D. A., Gonzalez, O. F., Douglas, J. G., and Kreisberg, J. I. 1988. *Biochem. J.* **251**, 907–912.
19. Kamm, K. E., Hsu, L. C., Kubota, Y., and Stull, J. T. 1989. *J. Biol. Chem.* **264**, 21223–21229.
20. Singer, H. A., Oren, J. W., and Benscoter, H. A. 1989. *J. Biol. Chem.* **264**, 21215–21222.
21. Nishizuka, Y. 1988. *Nature* **334**, 661–665.
22. Huwiler, A., Fabbro, D., and Pfeilschifter, J. 1991. *Biochem. J.* **279**, 441–445.